

# Fabrication of all solid-state rechargeable lithium battery and its electrochemical properties

Young Ho Rho<sup>a,b,1</sup>, Kiyoshi Kanamura<sup>a,b,\*</sup>

<sup>a</sup> Department of Applied Chemistry, Graduate School of Engineering, Tokyo Metropolitan University, 1-1 Minami-Ohsawa, Hachioji, 192-0397 Tokyo, Japan

<sup>b</sup> CREST, Japan Science and Technology Corporation, 4-1-8, Honcho Kawaguchi, 332-0012 Saitama, Tokyo, Japan

Received 8 October 2005; received in revised form 17 October 2005; accepted 18 October 2005

Available online 28 November 2005

## Abstract

An all solid-state rechargeable lithium battery was successfully fabricated using a ceramic electrolyte and a thin film technique. A polymer-modified sol–gel method was applied in order to prepare the electrode-coated ceramic electrolyte.  $\text{Li}_4\text{Ti}_5\text{O}_{12}$  known for its outstanding electrochemical performances and the partially crystallized glass ceramics,  $\text{LiTi}_2(\text{PO}_4)_3\text{-AlPO}_4$  were adopted as electrode and electrolyte materials, respectively. The all solid-state battery cell constructed with lithium metal, PMMA buffer, and electrode-coated ceramic electrolyte was electrochemically evaluated with ac impedance, cyclic voltammetry, and discharge–charge test. The impedance of the interface between  $\text{Li}_4\text{Ti}_5\text{O}_{12}$  film and the solid electrolyte showed a relatively low resistance of  $\sim 110 \Omega \text{ cm}^{-2}$  at 1.60 V. Highly reversible sharp redox peaks were observed at around 1.55 V from cyclic voltammograms, and these were still clear even at a high scan rate of  $3 \text{ mV s}^{-1}$ , indicating a fast electrochemical response. A charge–discharge experiment showed an excellent reversibility of the cell but a relatively smaller discharge capacity of  $100.49 \text{ mAh g}^{-1}$  at C/5 than theoretical one of  $175 \text{ mAh g}^{-1}$ . This may be due to formation of an interlayer at the interface, which may be caused by chemical reaction between  $\text{Li}_4\text{Ti}_5\text{O}_{12}$  and the ceramic electrolyte during a firing step during preparation. In spite of the undesirable side-reaction, the ceramic electrolyte was successfully applied to the solid-state rechargeable lithium battery by means of a thin film technique using the polymer-modified sol–gel method, through increasing the interfacial contact area, i.e. reducing the interfacial resistance.

© 2005 Elsevier B.V. All rights reserved.

**Keywords:** PVP sol–gel method; Oxide electrolyte; Ceramic electrolyte; Solid electrolyte; Lithium battery; Thin film battery

## 1. Introduction

Much interest has been paid to solving a safety problem on rechargeable lithium batteries. Research on non-liquid electrolyte systems, such as a gel-polymer electrolyte and a polymer electrolyte, have been performed and partly commercialized. However, they still involve a flammable liquid electrolyte to maintain their high ionic conductivity, and therefore the effort to solve the safety problem continues. This has encouraged many researchers to develop nonflammable ionic liquid and/or inorganic solid (ceramic) electrolytes [1–14]. Research on a

nonflammable ionic liquid electrolyte has just started and is a promising field for lithium rechargeable battery research [10–14], while the ceramic electrolyte field has been focused on by many research groups for a relatively long period [1–9]. In the case of ceramic electrolyte, a lithium ion conductivity of  $\sim 10^{-3} \text{ S cm}^{-1}$  is required for practical use to avoid undesirable high polarization during charge and discharge cycles. Some remarkable results on the ceramic electrolytes have been reported and applied to all solid-state rechargeable batteries without any liquid and/or organic component [1–3,7–9]. Nonetheless, air-stable electrolytes such as  $\text{Li}_{0.33}\text{La}_{0.55}\text{TiO}_3$  with a perovskite structure and  $\text{LiTi}_2(\text{PO}_4)_3\text{-AlPO}_4$  (LTP) with a NASICON type structure [4–6] have not succeeded in their application to batteries in spite of an outstanding ionic conductivity of  $\sim 10^{-3} \text{ S cm}^{-1}$ . In the present study, the air-stable ceramic electrolyte, LTP was applied to fabrication of a rechargeable lithium battery, and remarkable electrochemical results were obtained.

\* Corresponding author. Tel.: +81 426 77 2828; fax: +81 426 77 2828.

E-mail addresses: [yrho@uwaterloo.ca](mailto:yrho@uwaterloo.ca) (Y.H. Rho), [kanamura-kiyoshi@c.metro-u.ac.jp](mailto:kanamura-kiyoshi@c.metro-u.ac.jp) (K. Kanamura).

<sup>1</sup> Present address: Department of Chemistry, University of Waterloo, 200 University Avenue West, Waterloo, Ont., Canada N2L 3G1.

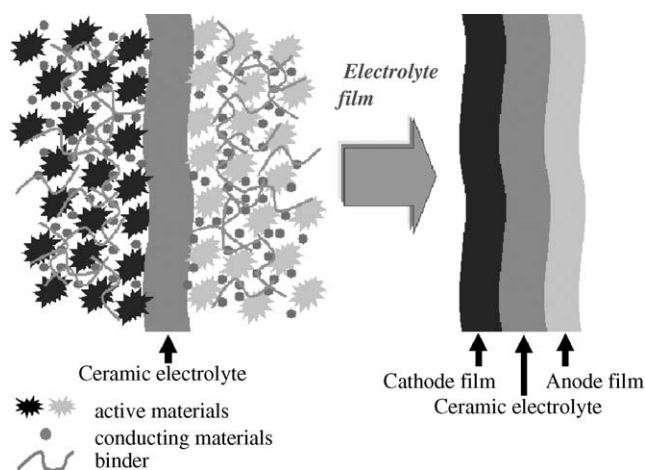


Fig. 1. Schematic interfacial area between electrode and electrolyte.

Before starting the research on the ceramic electrolyte, it should be noted that high resistance is generally produced due to an insufficient contact at the solid–solid interface between electrode and electrolyte. Therefore, for practical use, it is firstly required to increase the contact area between electrode and solid electrolyte in order to decrease the interfacial resistance. So far, many researchers have tried solving the poor contact problem at the solid–solid interface with many ideas, for example, high mechanical pressure. From a practical point of view, it sounds more reasonable to use thin film technology in order to solve the problem than to apply mechanical high pressure. As described in Fig. 1, thin film technology can help materials to be deposited onto a solid substrate with more compactness and a higher density. Our previous efforts for the development of thin film batteries [6,15–18], can be successfully applied as a promising method to increase the contact area at the interface between two solids, i.e. electrode and electrolyte. In this study,  $\text{Li}_4\text{Ti}_5\text{O}_{12}$  having been mentioned by many researchers as an alternate anode material for all solid-state rechargeable lithium batteries [15,16,18,19] was selected as the electrode material and the sol–gel method modified by an incorporation of poly(vinylpyrrolidone) (PVP) was successfully adapted not only for the thin film preparation but also for improvement of the electrochemical performance [5,15–18].

## 2. Experimental

$\text{Li-Ti-O}$  sol with poly(vinylpyrrolidone) (PVP) was synthesized as previously reported [4,5]. The molar composition of starting solutions was  $\text{Li}(\text{OC}_3\text{H}_7)_2:(\text{CH}_3)_2\text{CHO})_4\text{Ti}:\text{PVP}:\text{CH}_3\text{COOH}:\text{i-C}_3\text{H}_7\text{OH} = 4:5:5:100:100$ . Spin coating was conducted with a rotation speed of 3000 rpm in order to prepare a  $\text{Li-Ti-O}$  gel film on a ceramic electrolyte. The gel film was converted to a  $\text{Li}_4\text{Ti}_5\text{O}_{12}$  thin film after being fired at  $600^\circ\text{C}$  for 20 min. LTP sheet (Ohara glass) with 0.5 mm thickness provided from Ohara Inc. was used as the solid (ceramic) electrolyte which showed a high  $\text{Li}^+$  ion conductivity ( $8.2 \times 10^{-4} \text{ S cm}^{-1}$ ) as previously reported [4].

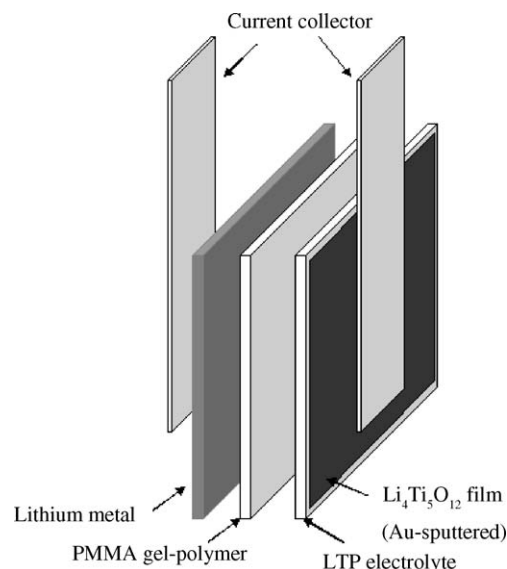


Fig. 2. Configuration of the all solid-state cell used in this study.

Impedance measurements were carried out in the frequency ranges of 100 kHz to 10 mHz. Cyclic voltammetry (CV) was also performed at various scan rates. The all solid-state cell was configured as a two-electrode system. The working electrode was  $\text{Li}_4\text{Ti}_5\text{O}_{12}$  coated on LTP solid electrolyte and the counter electrode was pure lithium metal. In order to avoid the undesirable reaction between LTP solid electrolyte and the lithium metal, poly(methyl methacrylate) (PMMA) gel-polymer electrolyte was used as a buffer layer, as described in Fig. 2. This polymer-type buffer electrolyte was used just to investigate the electrochemistry of the electrode-coated ceramic electrolyte and should be eliminated in practical applications. PMMA was prepared by thermal polymerization of methyl methacrylate monomer containing ethylene glycol dimethacrylate as the cross-linking agent. Azobisisobutyronitrile was used as a polymerization initiator and a liquid solution of ethylene carbonate and diethyl carbonate with  $1 \text{ mol dm}^{-3} \text{ LiClO}_4$  was used as the electrolyte. The thickness of the PMMA gel-polymer was  $300 \mu\text{m}$ . All of electrochemical experiments were conducted in an argon-filled glove box at room temperature.

## 3. Result and discussion

Fig. 3 shows the cyclic voltammogram of the  $\text{Li}_4\text{Ti}_5\text{O}_{12}$  thin film electrode prepared on a LTP solid electrolyte by using the PVP sol–gel method. The voltammogram was in good agreement with those reported in previous papers. In fact, similar voltammograms have been also published in our previous communication [15,16,18]. In all previous work, liquid electrolytes such as propylene carbonate, ethylene carbonate, and diethyl carbonate containing various lithium salts were utilized in the electrochemical cells.

Though the PMMA gel-polymer is unnecessary for the all solid-state cell, it was used as a buffer layer between LTP and lithium metal because it is not easy to electrochemically evaluate the electrode-coated ceramic electrolyte without

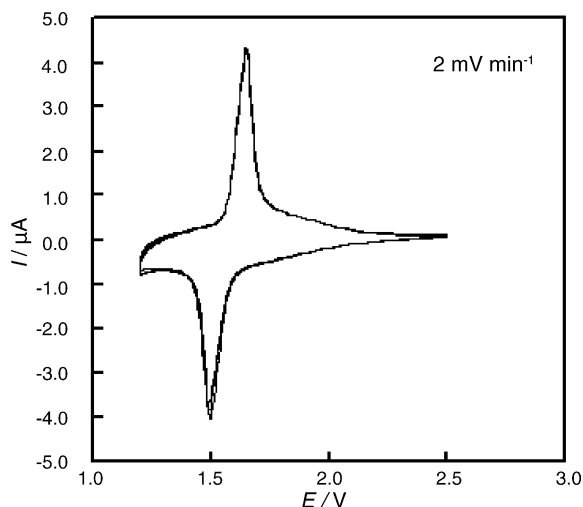


Fig. 3. Cyclic voltammogram of  $\text{Li}_4\text{Ti}_5\text{O}_{12}$  thin film electrode-coated LTP ceramic electrolyte ( $\text{Li}_4\text{Ti}_5\text{O}_{12}/\text{LTP}/\text{PMMA}/\text{Li}$ ) at a scan rate of  $2 \text{ mV min}^{-1}$ .

lithium metal as a counter electrode in the present technique. In other words, in order to investigate the electrochemical properties of the (one side) electrode-coated ceramic electrolyte without any complexity, it was temporarily required to use the PMMA gel-polymer electrolyte as a buffer in this study. Fig. 4 shows the impedance spectra of  $\text{Li}/\text{PMMA}/\text{Li}$  and  $\text{Li}/\text{PMMA}/\text{LTP}/\text{PMMA}/\text{Li}$  cells. A semi-circle was observed in Fig. 4(a), corresponding to  $\text{Li}^+$  ion conduction of PMMA gel-polymer electrolyte and a charge transfer resistance of Li metal/PMMA interface. However, the resistance of the PMMA gel electrolyte seems to be much larger than that of the charge transfer resistance, so that the semi-circle is mostly attributed to the resistance of the PMMA gel electrolyte. From the diameter of this semi-circle, the conductivity of PMMA gel electrolyte was estimated to be  $1.88 \times 10^{-4} \text{ S cm}^{-1}$ . This was in good agreement with that obtained by using a blocking electrode (Au). In the case of a  $\text{Li}/\text{PMMA}/\text{LTP}/\text{PMMA}/\text{Li}$  cell, two semi-circles were observed and each resistance was estimated to be 170 and  $80 \Omega$ . From a comparison of two impedance spectra, it can be seen that the semi-circle appeared in a high frequency region corresponding to the LTP solid electrolyte.

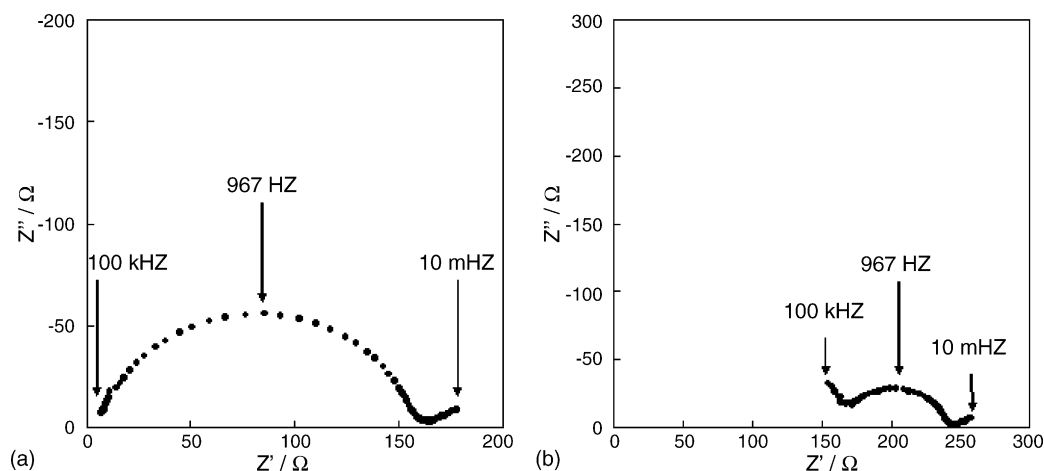


Fig. 4. Impedance spectra of (a)  $\text{Li}/\text{PMMA}/\text{Li}$  and (b)  $\text{Li}/\text{PMMA}/\text{LTP}/\text{PMMA}/\text{Li}$  cells.

Fig. 5 shows the impedance spectra of the all solid-state cell with a  $\text{Li}_4\text{Ti}_5\text{O}_{12}$  electrode/LTP electrolyte interface. From Fig. 4, it was shown that the semi-circles corresponding to the LTP and PMMA gel-polymer electrolyte appeared at high frequency ranges. An additional semi-circle was also shown between those of LTP and PMMA in the high frequency region. This can be explained as a result of chemical reactions between the LTP solid electrolyte and the  $\text{Li}_4\text{Ti}_5\text{O}_{12}$  solid electrode during firing. And a semi-circle observed in a low frequency region can be considered as an interfacial charge-transfer resistance (hereafter interfacial resistance) between  $\text{Li}_4\text{Ti}_5\text{O}_{12}$  and LTP (or interlayer). Therefore, the impedance appearing in Fig. 5 consists of the  $\text{Li}^+$  ion conductivity of the LTP electrolyte, the interlayer produced at between LTP and  $\text{Li}_4\text{Ti}_5\text{O}_{12}$  by the side-reaction, the PMMA gel-polymer electrolyte, and the interfacial resistance between  $\text{Li}_4\text{Ti}_5\text{O}_{12}$  and the LTP electrolyte (and/or interlayer). As a consequence, the resistance of the solid electrolyte for  $\text{Li}^+$  ion conduction was estimated to be  $230 \Omega$ . The interfacial resistance between  $\text{Li}_4\text{Ti}_5\text{O}_{12}$  and LTP electrolyte was  $370 \Omega$ . The overall value is sufficiently small at the initial voltage before the charge process, and this is due to the large contact area between  $\text{Li}_4\text{Ti}_5\text{O}_{12}$  and the LTP solid electrolyte. On the other hand, the undesirable interlayer from the side-reaction should be suppressed during the whole process even though the resistance was very small in order to properly operate the cell studied.

Fig. 6 shows the impedance spectra of Li metal/PMMA/LTP solid electrolyte/ $\text{Li}_4\text{Ti}_5\text{O}_{12}$  cell at various cell voltages between 1.86 and 1.60 V. When  $\text{Li}^+$  ions are intercalated into the  $\text{Li}_4\text{Ti}_5\text{O}_{12}$  electrode, the cell voltage is decreased due to reduction of Ti ions. The overall resistance estimated from the impedance spectra was decreased with the lowering cell voltage. The semi-circle in the high frequency region was not changed with cell voltage, but the semi-circle in the lower frequency region became smaller at the lower cell voltages. Therefore, it can be concluded that the former semi-circle is due to the impedance relating to  $\text{Li}^+$  ion conduction in the LTP solid electrolyte and the latter is due to a charge transfer resistance at the interface between the LTP solid electrolyte and  $\text{Li}_4\text{Ti}_5\text{O}_{12}$  electrode. The charge transfer resistance of the all solid-state cell

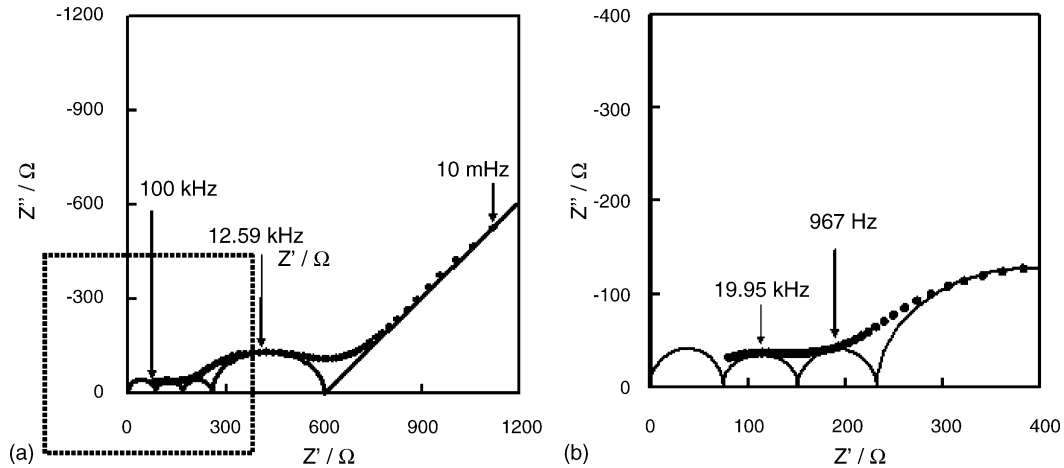


Fig. 5. Impedance spectra of Li/PMMA/LTP/Li<sub>4</sub>Ti<sub>5</sub>O<sub>12</sub> cell in (a) overall and (b) high frequency regions at an initial cell voltages.

was estimated to be  $140 \Omega \text{ cm}^{-2}$  at 1.60 V, whereas the interfacial resistance between Li<sub>4</sub>Ti<sub>5</sub>O<sub>12</sub> thin film and non-aqueous electrolyte has been estimated to be  $14 \Omega \text{ cm}^{-2}$  at 1.59 V [18]. The comparison of the two resistances shows that the interfacial resistance between the solid electrolyte and solid electrode is even larger than that between liquid electrolyte and solid electrode, indicating that further effort is needed for a ceramic type all solid-state battery.

In a battery system, a fast electrochemical response of cells is one of the important factors for good battery performance. In general, it is well known that an all solid-state battery has very poor discharge and charge properties at high current rates. Therefore, it is very difficult to fabricate all solid-state cells with fast electrochemical responses using a standard assembly technology. This is believed to be due to a high interfacial resistance between the active material and solid electrolyte. In this study, the electrochemical response at the interface between LTP and Li<sub>4</sub>Ti<sub>5</sub>O<sub>12</sub> was examined by cyclic voltammetry with relatively high scan rates. Fig. 7 shows the cyclic voltammograms of the all solid-state cell at various scan rates. Both cathodic and anodic peak currents were increased with increasing scan rate. Moreover, a peak separation between the cathodic and anodic peaks was also increased with the higher scan rate. This behavior is

ascribed to the ohmic drop due to the resistance of solid electrolyte and the interfacial resistance between solid electrode and solid electrolyte. Nonetheless, the redox peaks were still sharp even at a relatively high scan rate of  $3 \text{ mV s}^{-1}$ , indicating that the all solid-state cell had a fast electrochemical response. This sweep rate corresponds to more than 0.1 C discharge and charge rates. The LTP solid electrolyte used for our all solid-state electrochemical cell was relatively thick (0.5 mm). The thickness of the electrolyte can be thinner through several ways such as a thin film technology, so that when such a thin film electrolyte would be applied to our all solid-state electrochemical cell, improved electrochemical performance could be expected.

The charge and discharge test was also performed at a current density of  $5 \mu\text{A cm}^{-2}$ , which corresponds to a current rate of C/5. Fig. 8(a) shows the charge and discharge curves. The flat charge and discharge curve is a typical property of Li<sub>4</sub>Ti<sub>5</sub>O<sub>12</sub>. From those curves, it can be seen that the charge and discharge property is very reversible and the 1st discharge capacity is  $100.49 \text{ mAh g}^{-1}$ . The observed discharge capacity was smaller than the theoretical value of  $175 \text{ mAh g}^{-1}$ . The thickness of Li<sub>4</sub>Ti<sub>5</sub>O<sub>12</sub> was estimated to be  $0.15 \mu\text{m}$  by scanning electron microscope observation. A small discharge capacity may be due to some chemical reaction between LTP solid electrolyte and

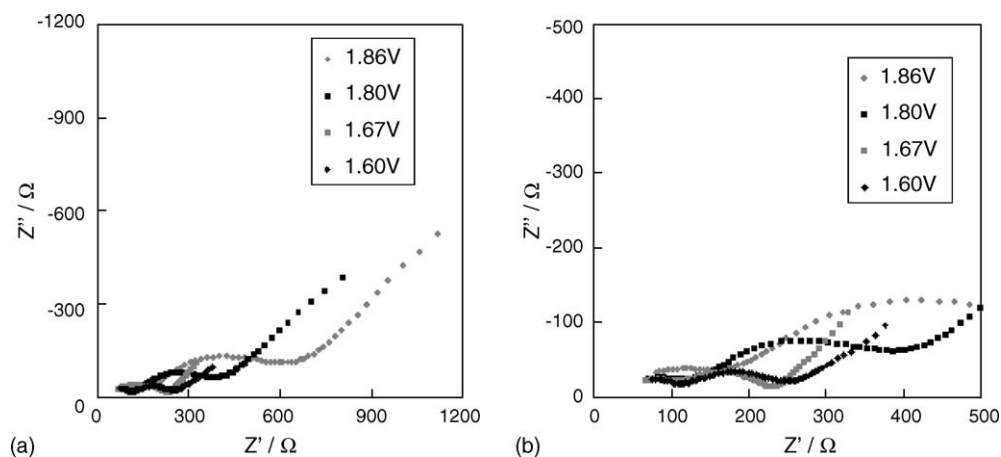


Fig. 6. Impedance spectra of Li/PMMA/LTP/Li<sub>4</sub>Ti<sub>5</sub>O<sub>12</sub> cell with various cell voltages.

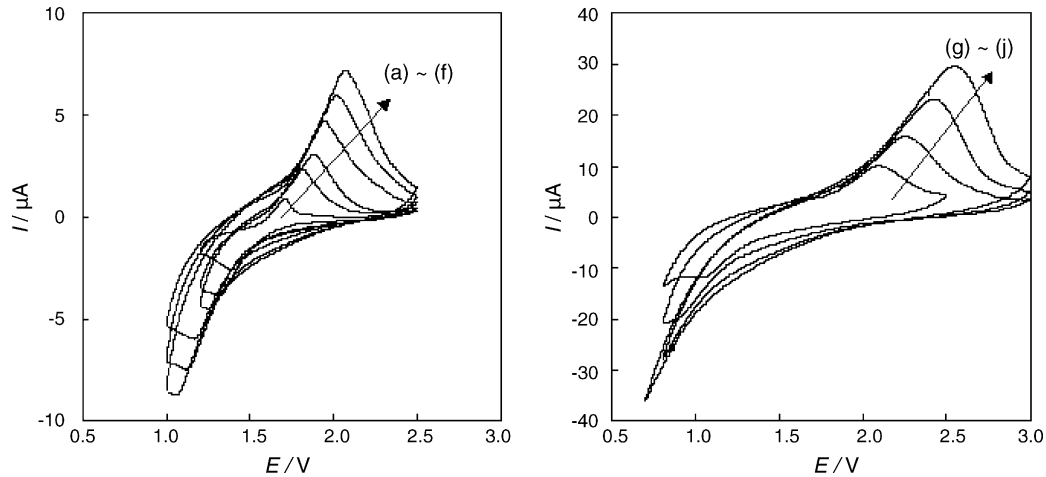


Fig. 7. Cyclic voltammograms of  $\text{Li}_4\text{Ti}_5\text{O}_{12}/\text{LTP}/\text{PMMA}/\text{Li}$  with various scan rates: (a)  $1 \text{ mV min}^{-1}$ , (b)  $4 \text{ mV min}^{-1}$ , (c)  $6 \text{ mV min}^{-1}$ , (d)  $10 \text{ mV min}^{-1}$ , (e)  $20 \text{ mV min}^{-1}$ , (f)  $30 \text{ mV min}^{-1}$ , (g)  $60 \text{ mV min}^{-1}$ , (h)  $120 \text{ mV min}^{-1}$ , and (i)  $180 \text{ mV min}^{-1}$ .

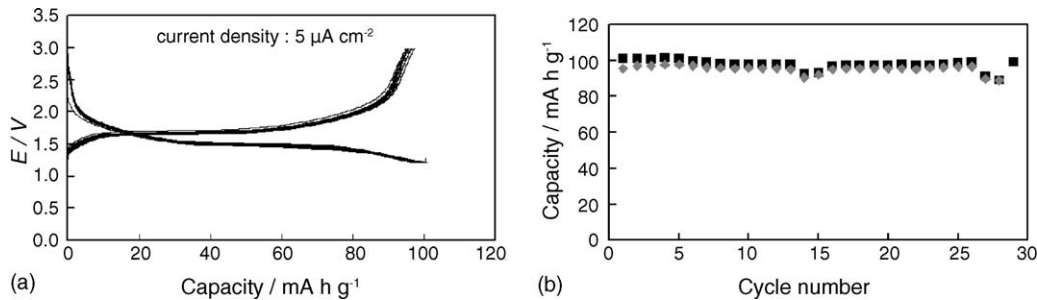


Fig. 8. (a) Discharge–charge curves and (b) cycle performance (■ charge, ♦ discharge) of  $\text{Li}_4\text{Ti}_5\text{O}_{12}/\text{LTP}/\text{PMMA}/\text{Li}$  cell at a current density of  $5 \mu\text{A cm}^{-2}$ .

$\text{Li}_4\text{Ti}_5\text{O}_{12}$  electrode material during firing as mentioned above, and some experimental error of the estimation of the film thickness. Of course, the heating condition can be also successfully explained as one reason of the capacity loss. Several conditions such as the heating temperature for the preparation of  $\text{Li}_4\text{Ti}_5\text{O}_{12}$  thin film used in liquid electrolyte system were previously investigated, and then the best condition was obtained at  $600^\circ\text{C}$  for 1 h [6]. Though the optimized condition was successfully applied to the preparation of electrode film on the glass ceramic electrolyte, an additional modification was required in order to avoid an undesirable reaction between electrode and electrolyte during firing. Consequently, the heating time shortened to 20 min, resulting in a small capacity loss.

Fig. 8(b) shows the cycle performance of the all solid-state cell. From this figure, the capacity fading due to damage of the  $\text{Li}_4\text{Ti}_5\text{O}_{12}$  matrix was rarely observed during cycling, meaning that the electrode film on LTP electrolyte was very stable. Of course, it is very well known that  $\text{Li}_4\text{Ti}_5\text{O}_{12}$  itself shows excellent cycleability due to the stability of the spinel framework and the minimal lattice expansion upon cycling [19].

#### 4. Conclusions

An all solid-state rechargeable lithium battery was successfully fabricated with a PVP-modified sol–gel method, and showed excellent electrochemical properties, i.e. a fast electrochemical responses, reversible charge and discharge cycling,

long cycle life, etc. In consequence, our thin film technique with a PVP-modified sol–gel method succeeded in making a thin electrode film on a ceramic electrolyte, decreasing the interfacial contact resistance by means of increasing the contact area between the ceramic solids. Therefore, the film preparation with the PVP-modified sol–gel method can be strongly recommended as a promising one in order to solve the interfacial contact problem between two ceramic solids (electrode and electrolyte).

#### References

- [1] N.J. Dudney, *J. Power Sources* 89 (2000) 176.
- [2] R. Kanno, T. Hata, Y. Kawamoto, M. Irie, *Solid State Ionics* 130 (2000) 97.
- [3] R. Kanno, M. Murayama, T. Inada, T. Kobayashi, K. Sakamoto, N. Sonoyama, A. Yamada, S. Kondo, *Electrochem. Solid State Lett.* 7 (2004) A455.
- [4] J. Fu, *J. Am. Ceram. Soc.* 80 (1997) 1901.
- [5] Y. Inaguma, C. Liqun, M. Itoh, T. Nakamura, T. Uchida, H. Ikuta, M. Wakihara, *Solid State Commun.* 86 (1993) 689.
- [6] K. Kanamura, T. Mitsui, Y.H. Rho, T. Umegaki, *Key Eng. Mater.* 228–229 (2002) 285.
- [7] N. Machida, H. Yamamoto, S. Asano, T. Shigematsu, *Solid State Ionics* 176 (2005) 473.
- [8] T. Ohtomo, F. Mizuno, A. Hayashi, K. Tadanaga, M. Tatsumisago, *J. Power Sources* 146 (2005) 715.
- [9] A. Hayashi, O. Takamasa, F. Mizuno, K. Tadanaga, M. Tatsumisago, *Electrochem. Commun.* 5 (2003) 701.
- [10] M. Holzapfel, C. Jost, P. Novák, *Chem. Comm.* 2004 (2004) 2098.
- [11] H. Sakaebe, H. Matsumoto, *Electrochem. Commun.* 5 (2003) 594.

- [12] P.C. Howlett, D.R. MacFarlane, A.F. Hollenkamp, *Electrochem. Solid State Lett.* 7 (2004) A97.
- [13] M. Egashira, S. Okada, J. Yamaki, D.A. Dri, F. Bonadies, B. Scrosati, *J. Power Sources* 138 (2004) 240.
- [14] B. Garcia, S. Lacallée, G. Perron, C. Michot, M. Armand, *Electrochim. Acta* 49 (2004) 4583.
- [15] Y.H. Rho, K. Kanamura, *J. Electrochem. Soc.* 150 (2003) A107.
- [16] Y.H. Rho, K. Kanamura, T. Umegaki, *Chem. Lett.* 2001 (2001) 1322.
- [17] Y.H. Rho, K. Kanamura, M. Fujisaki, J. Hamagami, S. Suda, T. Umegaki, *Solid State Ionics* 151 (2002) 151.
- [18] Y.H. Rho, K. Kanamura, *J. Solid. State. Chem.* 177 (2004) 2094.
- [19] T. Ohzuku, A. Ueda, N. Yamamoto, *J. Electrochem. Soc.* 142 (1995) 1431.